assumed for the 11p15.5 imprinted regions including the *IGF2–H19* domain on the basis of SRS or Beckwith–Wiedemann syndrome (BWS) phenotype in patients with multilocus hypomethylation[16] and BWS-like phenotype in patients with a upid (AC)pat cell lineage,[17] a mirror image of a upid(AC)mat cell lineage), (4) expression levels of imprinted genes in upid(AC)mat cells (although *SNRPN* expression of this patient was consistent with upid(AC)mat cells being predominant in leukocytes, complicated expression patterns have been identified for several imprinted genes in androgenetic and parthenogenetic fetal mice, probably because of perturbed *cis*- and *trans*-acting regulatory mechanisms)[18] and (5) unmasking of possible maternally inherited recessive mutation(s) in upid(AC)mat cells.[19] Collectively, it appears that the extent of overall (epi)genetic aberrations exceeded the threshold level for the development of SRS phenotype and horseshoe kidney characteristic of TS[4] but remained below the threshold level for the occurrence of other imprinting disorders or recessive Mendelian disorders.

In summary, we identified a upid(AC)mat 46,XX cell lineage in a woman with an SRS-like phenotype and a 45,X cell lineage accompanied by autosomal haploid sets of biparental origin. This report will facilitate further identification of patients with a upid(AC)mat cell lineage and better clarification of the clinical phenotypes in such patients.

Acknowledgements We thank the patient and her family members for their participation in this study. We also thank Dr. Toshiro Nagai for providing us with blood samples of patients with Prader–Willi syndrome.

Funding This work was supported by grants from the Ministry of Health, Labor, and Welfare and from the Ministry of Education, Science, Sports and Culture.

Competing interests None.

Patient consent Obtained.

Ethics approval This study was conducted with the approval of the Institutional Review Board Committees at National Center for Child health and Development.

Contributors Drs Kazuki Yamazawa (first author) and Kazuhiko Nakabayashi (second author) contributed equally to this work.

Provenance and peer review Not commissioned; externally peer reviewed.

REFERENCES

1. **McGrath J,** Solter D. Completion of mouse embryogenesis requires both the maternal and paternal genomes. *Cell* 1984;**37**:179–83.
2. **Strain L,** Warner JP, Johnston T, Bonthron DT. A human parthenogenetic chimaera. *Nat Genet* 1995;**11**:164–9.
3. **Horike S,** Ferreira JC, Meguro-Horike M, Choufani S, Smith AC, Shuman C, Meschino W, Chitayat D, Zackai E, Scherer SW, Weksberg R. Screening of DNA methylation at the H19 promoter or the distal region of its ICR1 ensures efficient detection of chromosome 11p15 epimutations in Russell–Silver syndrome. *Am J Med Genet Part A* 2009;**149A**:2415–23.
4. **Styne D,** Grumbach M. Puberty: ontogeny, neuroendocrinology, physiology, and disorders. In: Kronenberg H, Melmed M, Polonsky K, Larsen P, eds. *Williams textbook of endocrinology*, 11th edn. Philadelphia: Saunders 2008:969–1166.
5. **Thiede C,** Prange-Krex G, Freiberg-Richter J, Bornhauser M, Ehninger G. Buccal swabs but not mouthwash samples can be used to obtain pretransplant DNA fingerprints from recipients of allogeneic bone marrow transplants. *Bone Marrow Transplant* 2000;**25**:575–7.
6. **Brena RM,** Auer H, Kornacker K, Hackanson B, Raval A, Byrd JC, Plass C. Accurate quantification of DNA methylation using combined bisulfite restriction analysis coupled with the Agilent 2100 Bioanalyzer platform. *Nucleic Acids Res* 2006;**34**:e17.
7. **Yamazawa K,** Kagami M, Nagai T, Kondoh T, Onigata K, Maeyama K, Hasegawa T, Hasegawa Y, Yamazaki T, Mizuno S, Miyoshi Y, Miyagawa S, Horikawa R, Matsuoka K, Ogata T. Molecular and clinical findings and their correlations in Silver–Russell syndrome: implications for a positive role of IGF2 in growth determination and differential imprinting regulation of the IGF2-H19 domain in bodies and placentas. *J Mol Med* 2008;**86**:1171–81.
8. **Yamazawa K,** Kagami M, Ogawa M, Horikawa R, Ogata T. Placental hypoplasia in maternal uniparental disomy for chromosome 7. *Am J Med Genet Part A* 2008;**146A**:514–16.
9. **Abu-Amero S,** Monk D, Frost J, Preece M, Stanier P, Moore GE. The genetic aetiology of Silver–Russell syndrome. *J Med Genet* 2008;**45**:193–9.
10. **Eggermann T,** Eggermann K, Schonherr N. Growth retardation versus overgrowth: Silver–Russell syndrome is genetically opposite to Beckwith–Wiedemann syndrome. *Trends Genet* 2008;**24**:195–204.
11. **Goto T,** Monk M. Regulation of X-chromosome inactivation in development in mice and humans. *Microbiol Mol Biol Rev* 1998;**62**:362–78.
12. **Nagy A,** Sass M, Markkula M. Systematic non-uniform distribution of parthenogenetic cells in adult mouse chimaeras. *Development* 1989;**106**:321–4.
13. **Fundele R,** Norris ML, Barton SC, Reik W, Surani MA. Systematic elimination of parthenogenetic cells in mouse chimeras. *Development* 1989;**106**:29–35.
14. **Verp MS,** Rosinsky B, Le Beau MM, Martin AO, Kaplan R, Wallemark CB, Otano L, Simpson JL. Growth disadvantage of 45, X and 46, X, del(X)(p11) fibroblasts. *Clin Genet* 1988;**33**:277–85.
15. **Horsthemke B,** Wagstaff J. Mechanisms of imprinting of the Prader–Willi/Angelman region. *Am J Med Genet A* 2008;**146A**:2041–52.
16. **Azzi S,** Rossignol S, Steunou V, Sas T, Thibaud N, Danton F, Le Jule M, Heinrichs C, Cabrol S, Gicquel C, Le Bouc Y, Netchine I. Multilocus methylation analysis in a large cohort of 11p15-related foetal growth disorders (Russell Silver and Beckwith Wiedemann syndromes) reveals simultaneous loss of methylation at paternal and maternal imprinted loci. *Hum Mol Genet* 2009;**18**:4724–33.
17. **Wilson M,** Peters G, Bennetts B, McGillivray G, Wu ZH, Poon C, Algar E. The clinical phenotype of mosaicism for genome-wide paternal uniparental disomy: two new reports. *Am J Med Genet Part A* 2008;**146A**:137–48.
18. **Ogawa H,** Wu Q, Komiyama J, Obata Y, Kono T. Disruption of parental-specific expression of imprinted genes in uniparental fetuses. *FEBS Lett* 2006;**580**:5377–84.
19. **Engel E.** A fascination with chromosome rescue in uniparental disomy: Mendelian recessive outlaws and imprinting copyrights infringements. *Eur J Hum Genet* 2006;**14**:1158–69.

Epilepsia, 51(7):1259–1265, 2010
doi: 10.1111/j.1528-1167.2009.02495.x

FULL-LENGTH ORIGINAL RESEARCH

Interictal cerebral blood flow abnormality in cryptogenic West syndrome

***Shin-ichiro Hamano, †Norimichi Higurashi, *Reiko Koichihara, *Tomotaka Oritsu, *Kenjiro Kikuchi, †Satoshi Yoshinari, *Manabu Tanaka, and ‡Motoyuki Minamitani**

*Division of Neurology, Saitama Children's Medical Center, Saitama, Japan; †Department of Pediatrics, The Jikei University School of Medicine, Tokyo, Japan; and ‡Department for Child Health and Human Development, Saitama Children's Medical Center, Saitama, Japan

Summary

Purpose: To elucidate the abnormality of interictal regional cerebral blood flow (rCBF) of West syndrome at the onset.

Methods: Quantitative measurement of rCBF with an autoradiography method using *N*-isopropyl-(^{123}I) p-iodoamphetamine single photon emission computed tomography (SPECT) was performed on 14 infants with cryptogenic West syndrome. Regions of interest (ROIs) for rCBF were placed automatically using an automated ROI analysis software (three-dimensional stereotactic ROI template), and were grouped into 12 segments: callosomarginal, precentral, central, parietal, angular, temporal, posterior cerebral, pericallosal, lenticular nucleus, thalamus, hippocampus, and cerebellum. We compared rCBF between the patients and seven age-matched infants with cryptogenic focal epilepsy as a control group. The patients were divided into two groups according to the duration from onset to SPECT, to compare rCBF.

Results: Quantitative analysis revealed cerebral hypoperfusion in cryptogenic West syndrome with normal SPECT images under visual inspection. In bilateral central, posterior cerebral, pericallosal, lenticular nucleus, and hippocampus, and in the left parietal, temporal, and cerebellum, and in the right angular and thalamus segments there were statistical differences ($p < 0.05$). Compared with the duration from onset to SPECT, there were no significant differences of rCBF in all segments.

Discussion: Broad cerebral hypoperfusion with posterior predominance involving the hippocampus and lenticular nucleus implies that even cryptogenic West syndrome has a widespread cerebral dysfunction at least transiently, which would correspond to clinical manifestations of hypsarrhythmia and epileptic spasms. Hippocampal hypoperfusion suggests the dysfunction of hippocampal circuitry in the brain adrenal axis, and may contribute to subsequent cognitive impairment of cryptogenic West syndrome.

KEY WORDS: ^{123}I-iodoamphetamine, Cerebral metabolism, Development, Hypsarrhythmia, Infantile spasms, Three-dimensional stereotactic ROI template.

West syndrome is severe epileptic encephalopathy of infancy consisting of epileptic spasms and the characteristic electroencephalographic pattern called hypsarrhythmia, and is classified into symptomatic and cryptogenic types. Cryptogenic West syndrome shows normal development before onset, and also displays no brain abnormality according to structural neuroimaging examination. However, even in the patients with the cryptogenic type, almost half demonstrate moderate to severe mental retardation during long-term follow-up (Koo et al., 1993; Ito et al., 2002; Hamano et al., 2003).

Neurofunctional imaging studies have revealed that a subset of patients with West syndrome had focal abnormalities of the cerebral cortex (Chugani et al., 1990, 1992; Maeda et al., 1994; Haginoya et al., 1998, 2000; Munakata et al., 2004; Kakisaka et al., 2009). These studies proposed an important role of those focal abnormalities of the cerebral cortex in the pathophysiology and the development of West syndrome. Focal cortical abnormalities of neurofunctional imaging indicated subtle focal brain lesions, which probably provoke epileptic spasms through cortical–subcortical interaction (Chugani et al., 1990; Haginoya et al., 2000). Some of the localized cerebral dysfunction seems to contribute to mental retardation (Maeda et al., 1994). These authors demonstrated that the localized cortical abnormalities were transient and changed with the clinical symptoms, by visual

Accepted November 18, 2009; Early View publication February 1, 2010.

Address correspondence to Shin-ichiro Hamano, MD, PhD, Division of Neurology, Saitama Children's Medical Center, 2100 Magome, Iwatsuki-ku, Saitama, Saitama 339-8551, Japan. E-mail: hamano.shinichiro@pref.saitama.lg.jp

inspections of positron emission tomography (PET), and concluded that these functional abnormalities of the cerebral cortex may be associated with the development of the clinical manifestations of West syndrome.

We previously studied the alteration of the regional cerebral blood flow (rCBF) by adrenocorticotropic hormone (ACTH) therapy using single photon emission computed tomography (SPECT) (Hamano et al., 2007). Our quantitative analysis could not reveal the differences of the rCBF between the patients with cryptogenic West syndrome before ACTH therapy and the controls. Manual determination of regions of interest (ROIs) and unmeasured broad regions outside of ROIs might be disadvantages of the previous study. Therefore, our present study of the rCBF of 14 patients with cryptogenic West syndrome used *N*-isopropyl-(^{123}I) p-iodoamphetamine (IMP)-SPECT and fully automated ROI analysis software instead of manual determination of ROIs to reveal quantitatively the abnormality of rCBF associated with the clinical symptoms of West syndrome and the duration of the appearance of epileptic spasms and hypsarrhythmia.

Methods

The subjects of the present study were 14 infants (eight male and six female) with cryptogenic West syndrome. Cryptogenic West syndrome in this study was defined according to the following criteria: (1) clusters of epileptic spasms with onset <3 years; (2) hypsarrhythmia on electroencephalography (EEG); (3) normal pregnancy, normal development, and no eventful past history, including no other type of seizures before onset of spasms; (4) no focal abnormality on neurologic examinations; (5) normal brain images on computed tomography (CT) and magnetic resonance imaging (MRI); and (6) no focal abnormality and asymmetry of IMP-SPECT images. The mean onset age of the epileptic spasms of the 14 patients was 6.4 ± 2.5 [mean ± standard deviation (SD)] months, ranging from 3.0–10.0 months (information of seizure onset was obtained from the patients' parents). Investigations were performed on every patient to detect the etiologic factors of West syndrome. These included neurologic examinations, ophthalmologic examinations, EEG, brain CT and MRI, biochemical and metabolic tests including urine amino acids and organic acids, and chromosomal analysis.

SPECT examinations were performed before ACTH therapy or antiepileptic medications except pyridoxal phosphate. The age of patients at SPECT study was 9.3 ± 3.3 (mean ± SD), ranging from 3.7–16.5 months, and the duration from the onset to SPECT was 3.0 ± 3.2 (mean ± SD), ranging from 0.4–11.8 months. Quantitative measurement of rCBF was conducted with the autoradiography (ARG) method developed by Iida et al. (Iida et al., 1994). A triple-head gamma camera (Siemens Multispect 3, Siemens Medical Systems Inc., Hoffman Estates, IL, U.S.A.) was equipped with a fan beam collimator, and data were acquired with a 128 × 128 matrix for 120 degrees and 24 min in five-degree steps of 60 s per frame. In data processing, Siemens Icon-P was used for reconstruction of SPECT images, and a Butterworth filter and absorption correction (Chang, $\mu = 0.1$ cm^{-1}) were used to produce scanning images with an OM line and 256 × 256 matrix (1.2 mm/pixel). For all patients ^{123}I-IMP was injected intravenously at a dose of 55.5 megabecquerel (MBq) during their interictal periods ≥30 min after their last seizures. On all patients SPECT scanning was performed during sleep, and triclofos sodium, chloral hydrate, or pentobarbital calcium was used as a sedative. A 24-min scan was performed at 40 and 180 min (early image center time and late image center time, respectively). Approximately 10 min after intravenous injection of ^{123}I-IMP, arterial blood was collected from the opposite side of the ^{123}I-IMP infusion, and whole-blood radioactivity concentration was measured using a well-type scintillation counter. Obtained cross-calibration factors were input to determine quantitative measurements of rCBF. Thyroid block for radioactivity was performed by oral administration of Lugol's solution in a dose of two drops for 4 days, from 2 days before the SPECT examination.

We adopted fully automated ROI analysis software developed by Takeuchi et al., named three-dimensional stereotactic ROI template (3DSRT) (Takeuchi et al., 2003, 2004, 2006). This software is available free on Windows at any facility and is used by many clinicians to investigate rCBF quantitatively for adults and children (Ito et al., 2005; Kobayashi et al., 2008; Tateno et al., 2008; Kimura et al., 2009; Nagasawa et al., 2009). The SPECT images were anatomically standardized using statistical parametric mapping 99 followed by quantification of 318 ROIs unilaterally, grouped into 12 segments: callosomarginal, precentral, central, parietal, angular, temporal, posterior cerebral, pericallosal, lenticular nucleus, thalamus, hippocampus, and cerebellum (Fig. 1).

The SPECT data of seven age-matched epileptic infants with focal seizures were used as a control for comparison with the infants with cryptogenic West syndrome. They had a diagnosis of focal epilepsy; however, their interictal SPECT images were visually symmetric in distribution of CBF, their brain MRIs were normal, they had no focal neurologic deficits, and their development at the age of 3 years was normal. The seven infants comprised four boys and three girls, and their mean age at SPECT study was 10.1 ± 5.6 (mean ± SD), ranging from 3.1–17.7 months. Those variables were not significantly different from the values of the 14 patients with cryptogenic West syndrome. The SPECT procedure was similar to that described earlier.

Furthermore, to reveal the influences on cerebral blood flow by lasting epileptic spasms and hypsarrhythmia, the patients with West syndrome were divided into two groups by the duration from the onset to SPECT examination (<2 or ≥2 months). Demographic variables of the two groups were

Epilepsia, 51(7):1259–1265, 2010
doi: 10.1111/j.1528-1167.2009.02495.x

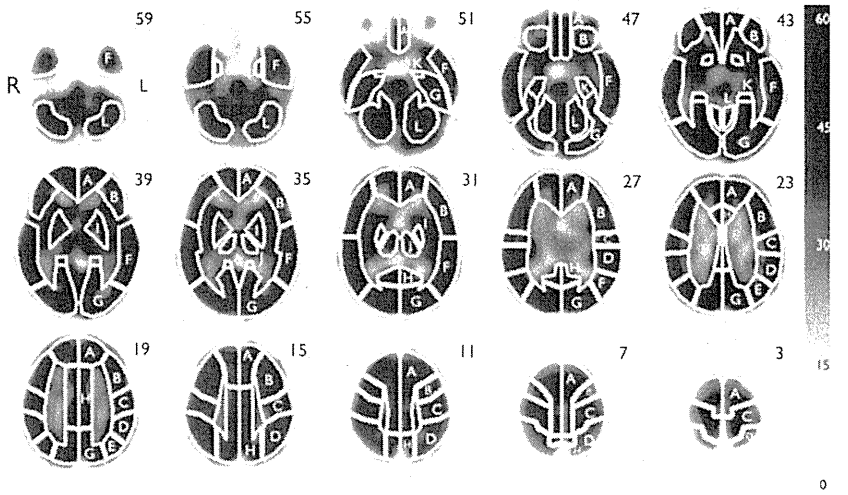

Figure 1.
The delineation of each segment of three-dimensional stereotactic region of interest template on the ^{123}I –iodoamphetamine single photon emission computed tomography (SPECT) image (**A**) callosomarginal segment, (**B**) precentral segment, (**C**) central segment, (**D**) parietal segment, (**E**) angular segment, (**F**) temporal segment, (**G**) posterior cerebral segment, (**H**) pericallosal segment, (**I**) lenticular nucleus segment, (**J**) thalamus segment, (**K**) hippocampus segment, (**L**) cerebellum segment.
Epilepsia © ILAE

not significantly different from each other except with regard to duration from the onset to SPECT (Table 1).

All SPECT examinations were performed in accordance with the policies of the Saitama Children's Medical Center Institutional Steering Committee, and informed consent was obtained from the parents.

The Mann-Whitney *U* test or Fisher's exact probability test was used for statistical analysis. Differences were considered statistically significant with a p-value of 0.05 or less.

Results

The rCBF values of the patients with cryptogenic West syndrome were lower than those of the control group in each corresponding segment (Table 2). In bilateral central, posterior cerebral, pericallosal, lenticular nucleus, and hippocampus segments; in the left parietal, temporal, and cerebellum segments; and in the right angular, and thalamus segments, there were statistically significant differences of the rCBF values ($p < 0.05$). The mean values of rCBF of West syndrome ranged from 35.6 (the right hippocampus segment) to 46.6 (the left thalamus segment) ml/100 g/min, and those of the control group ranged from 41.1 (the left hippocampus segment) to 54.6 (both sides of the lenticular nucleus segments) ml/100 g/min. The rCBF distribution patterns of the cryptogenic West syndrome group were similar to those of the control group, which indicated that the rCBF values in the central, angular, posterior cerebral, lenticular nucleus, and thalamus segments were higher than those in other regions in both groups, which ranged from 40–47 ml/100 g/min (West syndrome) and 48–55 ml/100 g/min (control). There were no statistically significant differences between the right and the left sides in each segment in the patients with West syndrome, and also in the control group.

Table 1. Demographic variables of two groups of the cryptogenic West syndrome divided by the duration from the onset to SPECT (<2 or ≥2 months)

	Duration from onset to SPECT		
	<2 months (n = 7)	≥2 months (n = 7)	p-value
Boy : girl	3:4	5:2	n.s.
Onset age of spasms in months, mean ± SD (range)	6.9 ± 2.9 (3.0–10.4)	5.9 ± 2.2 (3.6–10.0)	n.s.
Age at SPECT in months, mean ± SD (range)	7.7 ± 2.9 (3.7–11.6)	10.9 ± 3.0 (6.9–16.5)	n.s.
Duration from onset to SPECT in months, mean ± SD (range)	0.9 ± 0.5 (0.4–1.97)	5.0 ± 3.4 (2.4–11.8)	**

**$p < 0.01$.
n.s., not significant statistically between two groups; SPECT, single photon emission computed tomography.

Table 2. Regional cerebral blood flow (rCBF) in 12 segments of cryptogenic West syndrome compared with those of control group

Segment		Side	West syndrome (n = 14) rCBF in ml/100 g/min (mean ± SD)	Control (n = 7) rCBF in ml/100 g/min (mean ± SD)	p-value
A	Callosomarginal	R	36.8 ± 8.2	43.6 ± 8.2	n.s.
		L	36.6 ± 7.9	43.7 ± 9.2	n.s.
B	Precentral	R	39.5 ± 8.3	47.0 ± 9.3	n.s.
		L	38.5 ± 8.5	47.0 ± 8.9	n.s.
C	Central	R	40.4 ± 8.0	48.9 ± 9.2	*
		L	40.2 ± 8.6	49.6 ± 9.8	*
D	Parietal	R	39.6 ± 7.9	48.1 ± 11.3	n.s.
		L	38.6 ± 7.6	47.9 ± 11.9	*
E	Angular	R	40.8 ± 8.6	50.9 ± 11.5	*
		L	40.4 ± 8.5	51.0 ± 11.9	n.s.
F	Temporal	R	37.2 ± 7.2	45.3 ± 9.2	n.s.
		L	35.9 ± 7.8	44.6 ± 9.0	*
G	Posterior cerebral	R	42.3 ± 8.3	52.0 ± 8.9	*
		L	41.9 ± 8.1	51.5 ± 8.7	*
H	Pericallosal	R	40.2 ± 8.1	49.0 ± 8.8	*
		L	39.7 ± 8.0	49.0 ± 9.9	*
I	Lenticular nucleus	R	44.9 ± 8.5	54.6 ± 10.3	*
		L	45.3 ± 8.0	54.6 ± 9.7	*
J	Thalamus	R	44.0 ± 7.6	53.5 ± 11.4	*
		L	46.6 ± 8.8	53.7 ± 8.3	n.s.
K	Hippocampus	R	35.6 ± 6.6	41.7 ± 5.1	*
		L	35.7 ± 7.9	41.1 ± 4.7	*
L	Cerebellum	R	37.1 ± 6.6	43.5 ± 6.9	n.s.
		L	37.3 ± 6.4	44.4 ± 6.9	*

*$p < 0.05$.
n.s., not significant statistically between two groups; R, right; L, left; SD, standard deviation.

To reveal the influences on cerebral blood flow by lasting epileptic spasms and hypsarrhythmia, rCBFs were compared between the two groups of patients with cryptogenic West syndrome divided by the duration from the onset to SPECT examination (<2 or ≥2 months). There were no significant differences of rCBF between the two groups in all segments (Table 3).

Discussion

This quantitative study revealed a decrease of rCBF by 15–20% in the patients with cryptogenic West syndrome, in broad regions from central to occipital regions involving the lenticular nucleus and hippocampus, compared with the patients with cryptogenic focal epilepsy. To the best of our knowledge, this is the first report that has revealed hippocampal hypoperfusion in the early period of West syndrome by quantitative cerebral blood flow analysis using SPECT. Baram and Hatalski (1998) proposed the brain adrenal axis hypothesis concerning the pathophysiology of West syndrome. They suggested that corticotropin releasing hormone (CRH)–expressing γ-aminobutyric acid (GABA)ergic interneurons of the hippocampus might be influenced by stress-evoked excessive release of CRH from the amygdala via the entorhinal cortex. Hippocampal hypoperfusion may indicate hippocampal dysfunction associated with excessive CRH, and will be concordant with the brain adrenal axis hypothesis. Steroids normally exert a negative feedback on the production of CRH in the hypothalamus directly and via the hippocampus. Hippocampal dysfunction can cause an inappropriate negative feedback on CRH and may lead to a vicious spiral. Riikonen and Amnell (1981) demonstrated frequent comorbidity of autism in West syndrome, and they suggested a close association between the limbic system and autism. Hippocampal hypoperfusion in the early period of West syndrome may be associated with autism as a comorbidity of West syndrome.

Electrophysiologic study revealed the important role of pre- and/or postcentral gyri in the pathophysiology of epileptic spasms (Asano et al., 2005). It was found that the pre- and/or postcentral gyri involvement of the fast wave bursts were associated with the severity of limb movement of epileptic spasms (Asano et al., 2005). Hypoperfusion of the bilateral central segments in our study may be a consequence of frequent epileptic spasms, with which the fast wave bursts were associated.

Our study showed significant rCBF decrease in the bilateral occipital regions, and the left temporal and parietal

Table 3. Regional cerebral blood flow (rCBF) of the cryptogenic West syndrome compared by the duration from the onset to SPECT

Segment		Side	Duration from onset to SPECT: <2 months (n = 7) rCBF in ml/100 g/min (mean ± SD)	Duration from onset to SPECT: ≥2 months (n = 7) rCBF in ml/100 g/min (mean ± SD)	p
A	Callosomarginal	R	36.9 ± 10.2	36.6 ± 6.5	n.s.
		L	36.5 ± 9.8	36.7 ± 6.2	n.s.
B	Precentral	R	39.6 ± 10.9	39.4 ± 5.6	n.s.
		L	39.0 ± 11.0	38.1 ± 6.1	n.s.
C	Central	R	40.8 ± 9.5	39.9 ± 6.9	n.s.
		L	40.9 ± 10.8	39.4 ± 6.6	n.s.
D	Parietal	R	39.4 ± 10.0	39.8 ± 5.8	n.s.
		L	38.6 ± 9.9	38.7 ± 5.1	n.s.
E	Angular	R	40.2 ± 10.7	41.5 ± 6.8	n.s.
		L	39.9 ± 11.1	40.9 ± 5.8	n.s.
F	Temporal	R	37.0 ± 8.3	37.3 ± 6.6	n.s.
		L	36.2 ± 9.6	35.5 ± 6.2	n.s.
G	Posterior cerebral	R	41.8 ± 10.2	42.8 ± 6.7	n.s.
		L	41.4 ± 10.3	42.3 ± 5.9	n.s.
H	Pericallosal	R	40.4 ± 10.2	39.9 ± 6.2	n.s.
		L	39.6 ± 10.1	39.7 ± 6.0	n.s.
I	Lenticular nucleus	R	45.7 ± 11.4	44.1 ± 5.0	n.s.
		L	45.7 ± 9.9	44.8 ± 6.3	n.s.
J	Thalamus	R	44.3 ± 10.1	43.7 ± 4.8	n.s.
		L	46.5 ± 11.8	46.7 ± 5.4	n.s.
K	Hippocampus	R	36.1 ± 7.6	35.1 ± 6.1	n.s.
		L	36.4 ± 10.2	34.9 ± 5.6	n.s.
L	Cerebellum	R	36.9 ± 7.5	37.4 ± 6.1	n.s.
		L	36.7 ± 7.4	38.0 ± 5.9	n.s.

n.s., not significant statistically between two groups; R, right; L, left; SD, standard deviation; SPECT, single photon emission computed tomography.

segments in the patients with cryptogenic West syndrome with normal SPECT images under visual inspection. PET studies frequently detected hypometabolism in the parietooccipital-temporal regions, and the dysfunction of those cortical regions is considered to be associated with the development of West syndrome (Chugani et al., 1990; Chiron et al., 1993; Maeda et al., 1994). Electrocorticography showed that the fast wave bursts associated with epileptic spasms involved cortical regions extensively and rapidly, at least in two lobes (Asano et al., 2005). The normal brain development proceeds from the sensorimotor cortex to parietooccipital cortices, and eventually attains frontal cortex (Yakovlev & Lecours, 1967; Chugani et al., 1987; Chiron et al., 1992; Kato & Okuyama, 1993; Yoshinari et al., 2006). The fast wave bursts associated with epileptic spasms may propagate easily to cerebral cortices, which develop earlier during infancy. The hypometabolism and the hypoperfusion in parietooccipital temporal regions may be the consequence of cerebral dysfunction by the propagation of the fast wave bursts, although we should consider an undetectable lesion such as microscopic cortical dysplasia, which shows normal MRI and abnormal findings in PET (Chugani et al., 1990). Transient hypometabolism in posterior cerebral cortices during the early period of West syndrome was not associated with developmental delay (Maeda et al., 1994). However, when patients with intractable epileptic spasms such as candidates for resective surgery showed bitemporal hypometabolism, their outcomes were particularly poor (Chugani et al., 1996). These findings seem to correspond to the concept that the hypometabolism and the hypoperfusion in the posterior regions are the consequence of cerebral dysfunction by the repetitive propagation of fast wave bursts.

Concerning subcortical structures, our study showed hypoperfusion in the bilateral lenticular nucleus and hippocampus also. Hippocampal hypometabolism was detected in the patients with intractable West syndrome and poor developmental outcome (Chugani et al., 1996). Influence to hippocampus by repetitive epileptic spasms may contribute to developmental outcome. However, abnormality of lenticular nucleus is controversial. Hypermetabolism of lenticular nucleus and brainstem in the patients with West syndrome was reported (Chugani et al., 1992, 1996). Although there would be differences in investigation such as cerebral blood flow and cerebral metabolism, there is remarkably close correlation. The opposite results may contribute to the differences of examination timing. SPECT was performed on the patients as soon as possible from their onset before treatment except vitamin B6 in our study; however, PET

was performed for the evaluation of resection surgery at various times in their study, when epileptic spasms had disappeared or changed to partial seizures in some patients. Other fluorodeoxyglucose (FDG)-PET studies, which were performed at the onset of spasms, showed cortical hypometabolism frequently in parietotemporooccipital regions without lenticular hypermetabolism (Maeda et al., 1994; Natsume et al., 1996). These results correspond to the results of our cerebral perfusion study by SPECT. Cerebral perfusion was examined qualitatively using SPECT on 40 patients with West syndrome (Haginoya et al., 2000). Hyperperfusion in the basal ganglia or in the brainstem was observed in only one patient. We consider that lenticular nuclei would be hypoperfused in cryptogenic West syndrome just after the onset at least, and may be hypometabolized similarly.

Prolonged hypsarrhythmia is considered to lead to subsequent cognitive impairment (Koo et al., 1993; Kivity et al., 2004). Some researchers consider hypsarrhythmia to be a kind of nonconvulsive status epilepticus (Lux, 2007). The duration of hypsarrhythmia and spasms probably affects hypometabolism and hypoperfusion. We also analyzed the differences of rCBF by the duration from onset to SPECT examination; however, there were no significant differences in any segments between the two groups divided by the duration, more than 2 months or less. One of the causes associated with absence of differences between the two groups would be due to limitations in performing examinations and in obtaining clinical information concerning onset and severity of symptoms. We were unable to obtain the exact duration of hypsarrhythmia. Electroencephalography could not be performed before the patients visited hospitals. We were able to obtain information about the onset of epileptic spasms from the patients' parents; however, it is difficult to obtain accurate information of spasm frequency and intensity during the first visit from the parents. Aggregate and expanse of electrical propagation in cluster of spasms, which affect seizure frequency and intensity, could change the severity of interictal hypoperfusion. Not only the duration from the onset and continuity of hypsarrhythmia, but also the frequency and intensity of epileptic spasms, may influence interictal rCBF in cryptogenic West syndrome. It would be important to discriminate between the effect by spasms and the effect by hypsarrhythmia, and further study needs to be done on subject patients with infantile spasms without hypsarrhythmia and/or hypsarrhythmia without infantile spasms.

Our study showed that widespread cerebral hypoperfusion with posterior predominance involved the hippocampus and lenticular nucleus in West syndrome. This result implies that even cryptogenic West syndrome would have a broad region of cerebral hypoperfusion, at least transiently, which would reflect widespread cerebral dysfunction. Hypsarrhythmia or epileptic spasms themselves probably contribute to developmental outcomes; however, where in the brain they have effect remains obscure. Hippocampal hypoperfusion suggests the dysfunction of hippocampal circuitry in the brain adrenal axis, and may lead to subsequent cognitive impairment such as autism.

Acknowledgments

This study was financially supported by the Kawano Masanori Memorial Foundation for the Promotion of Pediatrics. We thank Emeritus Professor Eric Johnson (Jichi Medical University, Tochigi, Japan) for his assistance with the preparation of the manuscript. We also thank Ms. E. Hamano for her constant encouragement and helpful advice. We confirm that we have read the Journal's position on ethical issues involved in publication and affirm that this report is consistent with those guidelines.

Disclosure

None of the authors has any conflict of interest to disclose.

References

Asano E, Juhász C, Shah A, Muzik O, Chugani DC, Shah J, Sood S, Chugani HT. (2005) Origin and propagation of epileptic spasms delineated on electrocorticography. *Epilepsia* 46:1086–1097.

Baram TZ, Hatalski CG. (1998) Neuropeptide-mediated excitability: a key triggering mechanism for seizure generation in the developing brain. *Trends Neurosci* 21:471–476.

Chiron C, Raynaud C, Maziere B, Zilbovicius M, Laflamme L, Masure MC, Dulac O, Bourguignon M, Syrota A. (1992) Changes in regional cerebral blood flow during brain maturation in children and adolescents. *J Nucl Med* 33:696–703.

Chiron C, Dulac O, Bulteau C, Nuttin C, Depas G, Raynaud C, Syrota A. (1993) Study of regional cerebral blood flow in West syndrome. *Epilepsia* 34:707–715.

Chugani HT, Phelps ME, Mazziotta JC. (1987) Positron emission tomography study of human brain functional development. *Ann Neurol* 22:487–497.

Chugani HT, Shields WD, Shewmon DA, Olson DM, Phelps ME, Peacock WJ. (1990) Infantile spasms: I. PET identifies focal cortical dysgenesis in cryptogenic cases for surgical treatment. *Ann Neurol* 27:406–413.

Chugani HT, Shewmon DA, Sankar R, Chen BC, Phelps ME. (1992) Infantile spasms: II. Lenticular nuclei and brain stem activation on positron emission tomography. *Ann Neurol* 31:212–219.

Chugani HT, Da Silva E, Chugani DC. (1996) Infantile spasms: III. Prognostic implications of bitemporal hypometabolism on positron emission tomography. *Ann Neurol* 39:643–649.

Haginoya K, Kon K, Takayanagi M, Yoshihara Y, Kato R, Tanaka S, Yokoyama H, Munakata M, Nagai M, Maruoka S, Yamazaki T, Abe Y, Iinuma K. (1998) Heterogeneity of ictal SPECT findings in nine cases of West syndrome. *Epilepsia* 39:26–29.

Haginoya K, Kon K, Yokoyama H, Tanaka S, Kato R, Munakata M, Yagi T, Takayanagi M, Yoshihara Y, Nagai M, Yamazaki T, Maruoka S, Iinuma K. (2000) The perfusion defect seen with SPECT in West syndrome is not correlated with seizure prognosis or developmental outcome. *Brain Dev* 22:16–23.

Hamano S, Tanaka M, Mochizuki M, Sugiyama N, Eto Y. (2003) Long-term follow-up study of West syndrome: differences of outcome among symptomatic etiologies. *J Pediatr* 143:231–235.

Hamano S, Yoshinari S, Higurashi N, Tanaka M, Minamitani M, Eto Y. (2007) Regional cerebral blood flow and developmental outcome in cryptogenic West syndrome. *Epilepsia* 48:114–119.

Iida H, Itoh H, Nakazawa M, Hatazawa J, Nishimura H, Onishi Y, Uemura K. (1994) Quantitative mapping of regional cerebral blood flow using iodine-123-IMP and SPECT. *J Nucl Med* 35:2019–2030.

Ito M, Aiba H, Hashimoto K, Kuroki S, Tomiwa K, Okuno T, Hattori H, Go T, Sejima H, Dejima S, Ikeda H, Yoshioka M, Kanazawa O, Kawamitsu T, Ochi J, Miki N, Noma H, Oguro K, Ozaki N, Tamamoto A, Matsubara T, Miyajima T, Fujii T, Konishi Y, Okuno T, Hojo H. (2002) Low-dose ACTH therapy for West syndrome: initial effects and long-term outcome. *Neurology* 58:110–114.

Ito H, Mori K, Hashimoto T, Miyazaki M, Hori A, Kagami S, Kuroda Y. (2005) Findings of brain 99mTc-ECD SPECT in high-functioning autism-3-dimensional stereotactic ROI template analysis of brain SPECT. *J Med Invest* 52:49–56.

Kakisaka Y, Haginoya K, Ishitobi M, Togashi N, Kitamura T, Wakusawa K, Sato I, Hino-Fukuyo N, Uematsu M, Munakata M, Yokoyama H, Iinuma K, Kaneta T, Higano S, Tsuchiya S. (2009) Utility of subtraction ictal SPECT images in detecting focal leading activity and understanding the pathophysiology of spasms in patients with West syndrome. *Epilepsy Res* 83:177–183.

Kato T, Okuyama K. (1993) Assessment of maturation and impairment of the brain by I-123 iodoamphetamine SPECT and MR imaging in children. *Showa Univ J Med Sci* 5:99–114.

Kimura N, Kumamoto T, Masuda T, Nomura Y, Hanaoka T, Hazama Y, Okazaki T, Arakawa R. (2009) Evaluation of the effect of thyrotropin releasing hormone (TRH) on regional cerebral blood flow in spinocerebellar degeneration using 3DSRT. *J Neurol Sci* 281:93–98.

Kivity S, Lerman P, Ariel R, Danziger Y, Mimouni M, Shinnar S. (2004) Long-term cognitive outcomes of a cohort of children with cryptogenic infantile spasms treated with high-dose adrenocorticotropic hormone. *Epilepsia* 45:255–262.

Kobayashi S, Tateno M, Utsumi K, Takahashi A, Saitoh M, Morii H, Fujii K, Teraoka M. (2008) Quantitative analysis of brain perfusion SPECT in Alzheimer's disease using a fully automated regional cerebral blood flow quantification software, 3DSRT. *J Neurol Sci* 264:27–33.

Koo B, Hwang PA, Logan WJ. (1993) Infantile spasms: outcome and prognostic factors of cryptogenic and symptomatic groups. *Neurology* 43:2322–2327.

Lux AL. (2007) Is hypsarrhythmia a form of non-convulsive status epilepticus in infant? *Acta Neurol Scand* 115(suppl 186):37–44.

Maeda N, Watanabe K, Negoro T, Aso K, Ohki T, Ito K, Kato T. (1994) Evolutional changes of cortical hypometabolism in West's syndrome. *Lancet* 343:1620–1623.

Munakata M, Haginoya K, Ishitobi M, Sakamoto O, Sato I, Kitamura T, Hirose M, Yokoyama H, Iinuma K. (2004) Dynamic cortical activity during spasms in three patients with West syndrome: a multichannel near-infrared spectroscopic topography study. *Epilepsia* 45:1248–1257.

Nagasawa N, Yamakado K, Yamada T, Nakanishi S, Ito M, Suzawa N, Kitano T, Takeda K. (2009) Three-dimensional stereotactic ROI template for measuring regional cerebral blood flow in 99mTc-ECD SPECT: comparison with the manual tracing method. *Nucl Med Commun* 30:155–159.

Natsume J, Watanabe K, Maeda N, Kasai K, Negoro T, Aso K, Nakashima S, Tadokoro M. (1996) Cortical hypometabolism and delayed myelination in West syndrome. *Epilepsia* 37:1180–1184.

Riikonen R, Amnell G. (1981) Psychiatric disorders in children with earlier infantile spasms. *Dev Med Child Neurol* 23:747–760.

Takeuchi R, Yonekura Y, Takeda SK, Fujita K, Konishi J. (2003) Fully automated quantification of regional cerebral blood flow with three-dimensional stereotaxic region of interest template: validation using magnetic resonance imaging – technical note. *Neurol Med Chir (Tokyo)* 43:153–162.

Takeuchi R, Matsuda H, Yoshioka K, Yonekura Y. (2004) Cerebral blood flow SPECT in transient global amnesia with automated ROI analysis by 3DSRT. *Eur J Nucl Med Mol Imaging* 31:578–589.

Takeuchi R, Sengoku T, Matsumura K. (2006) Usefulness of fully automated constant ROI analysis software for the brain: 3DSRT and FineSRT. *Radiat Med* 24:538–544.

Tateno M, Kobayashi S, Utsumi K, Morii H, Fujii K (2008) Quantitative analysis of the effects of donepezil on regional cerebral blood flow in Alzheimer's disease by using an automated program, 3DSRT. *Neuroradiology* 50:723–727.

Yakovlev PI, Lecours AR. (1967) The myelogenetic cycles of regional maturation of the brain: an overview. In Minkowski A (Ed.) *Regional development of the brain in early life*. Davis Co, Philadelphia, pp. 3–70.

Yoshinari S, Hamano S, Eda N, Sakamoto M, Takahashi Y. (2006) Development of Regional Cerebral Blood Flow during Childhood Studied with Iodine-123-IMP SPECT. *Jikeikai Med J* 53:87–92.

ELSEVIER

Gaucher Disease Patient With Myoclonus Epilepsy and a Novel Mutation

Asako Tajima, MD*,
Toya Ohashi, MD, PhD*†,
Shin-ichiro Hamano, MD, PhD*‡,
Norimichi Higurashi, MD*‡, and
Hiroyuki Ida, MD, PhD*,

The *N188S* mutation in Gaucher disease is associated with myoclonus epilepsy. We performed genetic analysis on a patient with progressive myoclonus epilepsy, who had received antiepileptic drugs for over 10 years. We detected *N188S/G199D* on the gene encoding glucocerebrosidase. Mutant proteins carrying each mutation were expressed in COS-1 cells (a commonly used cell line which derives from kidney cells of the African green monkey). Measurements of enzymatic activity and Western blotting analysis were performed. When residual activities were measured, glucocerebrosidase with the *N188S* mutation exhibited 50% activity of the wild type, and with *G199D*, 7.4%. Neither mutation influenced the stability of the enzyme protein. These data suggested a diagnosis of Gaucher disease for this patient, and indicated that *G199D* is a novel mutation.

Tajima A, Ohashi T, Hamano S, Higurashi N, Ida H. Gaucher disease patient with myoclonus epilepsy and a novel mutation. Pediatr Neurol 2010;42:65-68.

Introduction

Gaucher disease is the most prevalent lysosomal storage disease, and is caused by more than 200 mutations that produce abnormal glucocerebrosidase. Gaucher disease exhibits a wide range of phenotypes, most of which cannot be explained by a correlation with a specific genotype. Types 2 and 3 of Gaucher disease comprise the neuronopathic forms of the disease, and present various central nervous system manifestations. One of these manifestations is myoclonus epilepsy, and although it is rare, more Gaucher patients presenting with myoclonus epilepsy are found.

The myoclonus epilepsy evident in Gaucher disease and its relationship to the *N188S* mutation were discussed previously. The first report of *N188S* from Kim et al. suggested that this mutation might be a protective gene for neuronopathic forms of Gaucher disease such as the *N370S* mutation [1]. However, considering the results of other studies, *N188S* carriers retain the possibility to develop myoclonic seizures [2-4], although the exact correlation remains unknown.

We report on a 16-year-old girl with intractable epileptic seizures, including myoclonus, who was finally diagnosed as manifesting Gaucher disease. We detected *N188S/G199D* by sequencing and restriction fragment length polymorphism analysis. *G199D* is a novel mutation, and this study describes the genetic and functional analyses of these mutations.

Case Report

Patient

A 16-year-old girl with epileptic seizures and a diagnosis of Gaucher disease was referred to our institution for genetic analysis. She first presented with generalized seizures at age 1 year. An electroencephalogram and computed tomography of the brain produced normal results, and she was diagnosed as manifesting epilepsy. She did not exhibit other neurologic signs until age 5 years, when she presented with absence epilepsy. Developmental delay had become apparent by the time she entered primary school. Valproic acid was not effective for treating the absence seizures, and other anticonvulsants were used. Her seizures improved with valproic acid, ethosuximide, and clonazepam for a few years. At age 11 years, she began to manifest generalized tonic-clonic seizures that occurred more and more frequently. Action tremors had also appeared, followed by motor ataxia, myoclonus, and supranuclear gaze palsy, which together suggested progressive myoclonus epilepsy. Vertical supranuclear gaze palsy was initially evident. Horizontal ocular movement also became restricted at age 18 years. Myoclonus was easily induced by mere contact, which made it very difficult for her to walk, and the antiepileptic drugs no longer controlled her seizures. Phenobarbital was added, but the seizures continued. However, after the administration of piracetam, she could walk again. Upon her admission to the hospital at age 16 years for further examination and to establish a diagnosis, she could sit alone and was able to walk, using a wide-based gait, with support. On admission, hepatosplenomegaly and

From the *Department of Pediatrics, and †Department of Gene Therapy, Institute of DNA Medicine, Jikei University School of Medicine, Tokyo, Japan; and ‡Division of Neurology, Saitama Children's Medical Center, Saitama, Japan.

Communications should be addressed to:
Dr. Tajima; Department of Pediatrics, Jikei University School of Medicine; 3-25-8 Nishi-shinbashi, Minato-ku; Tokyo 105-8461, Japan.
E-mail: atajima@jikei.ac.jp
Received February 9, 2009; accepted August 12, 2009.

doi:10.1016/j.pediatrneurol.2009.08.007 • 0887-8994/10/$—see front matter

anemia were not evident. However, her platelet counts were low, at 9.9 × $10^4/\mu L$. The level of angiotensin-converting enzyme was 20.0 U/L (normal, 7.0-25.0 U/L), and her level of acid phosphatase was 10.6 U/L (normal, 5.9-14.0 U/L). No abnormal signal was evident according to magnetic resonance imaging of the brain. An electroencephalogram revealed mainly α-waves with diffuse polyspike bursts. The differential diagnosis for progressive cerebellar ataxia and myoclonus includes lysosomal disease. Therefore, pathologic observations of the bone marrow were essential. Bone marrow aspiration using light microscopy revealed cells with a "sandpaper" appearance that resembled Gaucher cells (Fig 1). Because these observations suggested a lysosomal disease, we acquired informed consent from the parents, and analyzed the activities of various enzymes related to lysosome. Glucocerebrosidase activity was reduced in fibroblasts, to about 26% of normal control levels. However, this residual activity was relatively high compared with that of a known patient with Gaucher disease. Usually, patients with Gaucher disease demonstrate less than 10% enzyme activity (Table 1). Gaucher disease was suspected, and a genetic analysis was performed to confirm the diagnosis, after receiving informed consent from the parents. Serum glucosylceramide and chitotriosidase measurements were not performed because they were not commercially available in Japan.

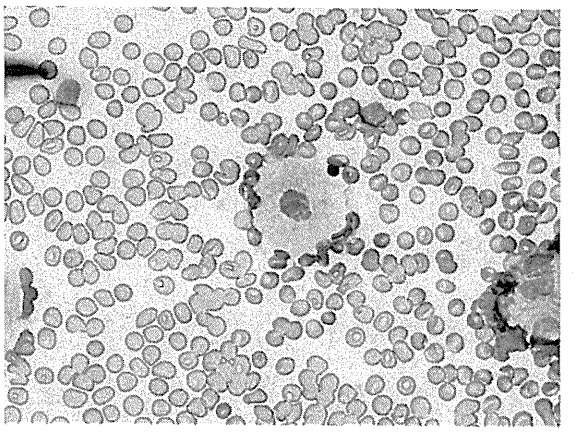

Figure 1. Light microscopy of a bone marrow aspiration (original magnification ×100). A cell with a "sandpaper" appearance was evident.

Genetic Analysis

We extracted DNA from white blood cells of the patient. Initially, eight common mutations in Gaucher disease (*N370S, L444P, F213I, 84GG, IVS2+1, D409H, R463C,* and *RecNciI*) were tested as described by Ida et al. [5-7]. However, because none of these mutations were identified, all exonic regions were amplified by polymerase chain reaction using Takara PCR Thermal Cycler (Takara Bio Inc., Otsu, Shiga, Japan), followed by single-strand conformation polymorphism analysis. Single-strand conformation polymorphism analysis revealed a shifted band in exon 6, and direct sequencing was performed using ABI Prism Model 3700 (Applied Biosystems, Foster City, CA). We identified *N188S* and *G199D* mutations in the same exon. Restriction fragment length polymorphism analysis was performed, and the polymerase chain reaction fragment was digested with *Tsp*RI or *Mbo*I to confirm the genotype. We also analyzed the parents' glucocerebrosidase gene, and learned that the parents carried both mutations heteroallelically.

Expression Analysis

To demonstrate that the two detected mutations caused reductions in glucocerebrosidase activity, mutant proteins carrying each of the mutations were produced. Each mutation was generated into glucocerebrosidase complementary DNA by using a QuikChange II Site-Directed Mutagenesis Kit (Stratagene, La Jolla, CA). The primers for exon 6 consisted of 5′-ATACCCCTGATTCACCGAGC-3′ (sense) and 5′-ACCCGGTCTAT GAAACACTT-3′ (antisense). After inserting the mutant complementary DNAs into pCDN6 plasmid, plasmids were transfected into COS-1, using Lipofectamine 2000 (Invitrogen, Carlsbad, CA).

After 48 hours, COS-1 cells were harvested, and glucocerebrosidase activities in the cells were measured using 4-methylumbelliferyl-β-glucopyranoside as a substrate, as described elsewhere [6]. The reaction was halted by adding 0.17 M glycine carbonate buffer (pH 10.4), and enzyme activity was measured by a spectrofluorophotometer, using RF-5300PC (Shimadzu, Tokyo, Japan). Residual glucocerebrosidase activities are described in Fig 2. Glucocerebrosidase activity was reduced in both mutants, and especially in the protein with *G199D*. The *N188S* mutant glucocerebrosidase demonstrated about 50% activity of the normal control, consistent with a previous report [8]. On the other hand, the *G199D*-bearing allele produced an enzyme with no significant activity. These results proved that *G199D* is a novel mutation that causes Gaucher disease, and the diagnosis of our patient was confirmed.

To determine whether glucocerebrosidase carrying the *N188S* or *G199D* mutation influenced protein stability, Western blotting analysis was performed. Proteins were subjected to sodium dodecyl sulfate polyacrylamide gel electrophoresis (10% polyacrylamide), and electrophoretically transferred onto nitrocellulose membranes. The membrane was blocked with 3% gelatin in Tris-buffered saline for 30 minutes, and washed with Tris-buffered saline containing 0.05% Tween-20. The membrane was then incubated with a polyclonal rabbit anti-glucocerebrosidase antibody for 1 hour at room temperature, and washed with Tris-buffered saline containing 0.05% Tween-20 (the antibody was produced by Toya Ohashi, MD, PhD, Department of Gene Therapy, Institute of DNA Medicine, Jikei University School of Medicine, Tokyo, Japan). After incubation with a goat anti-rabbit immunoglobulin G(H + L) alkaliphosphatase antibody (BioRad, Hercules, CA) for 1 hour, the membrane was washed with Tris-buffered saline containing 0.05% Tween-20 and Tris-buffered saline. The immunoreactive bands were detected using an AP Conjugate Substrate Kit (BioRad). The amounts of expressed proteins did not differ significantly (data not shown).

Discussion

In this study, we detected *N188S/G199D* in a glucocerebrosidase gene from a patient with myoclonus epilepsy. *G199D* was an unknown missense mutation, and therefore, to clarify its function and confirm that this mutation profoundly influences enzymatic activity, we performed Western blotting analysis and enzymatic analysis. Both experiments proved that *G199D* reduces glucocerebrosidase activity (7% of the wild type in this study) and leads to the onset of Gaucher disease. Moreover, the very low activity suggests that *G199D* is a null mutation. Although more cases are needed for confirmation, *G199D* is one of the mutations to be considered when evaluating a patient with Gaucher disease. On the other hand, *N188S* was previously demonstrated to exert a mild effect on glucocerebrosidase activity. Moreover, when *N188S* was expressed in COS-1 cells, enzymatic activity was only decreased to 50% of the wild type. Because of this relatively highly restored activity, we wondered whether *N188S* is really responsible for Gaucher disease. However, as we have mentioned, some patients with Gaucher disease and myoclonus epilepsy possess this mutation. Furthermore, we found cells resembling Gaucher cells in the bone marrow, indicating glucocerebroside accumulation in these cells.

Table 1. Residual activities of lysosomal enzymes (nmol/hr/mg)

	White Blood Cells		Fibroblast		
	Patient	Control (n = 3)	Patient	Control (n = 3)	GD* Patient
glucocerebrosidase	7.4	49.1 ± 2.2	470.0	1757 ± 653	53
beta-galactosidase	210.1	234 ± 2.5	1135.0	1213 ± 529	1120
hexosaminidase	6085.0	7032.3 ± 901.3	33757.0	32760 ± 17225	20360

Abbreviation:
GD = Gaucher disease

In view of these observations, *N188S* may be a gene responsible for Gaucher disease. However, to reach a final conclusion, we should confirm glucocerebroside accumulation in tissues biochemically, as well as morphologic changes.

At least seven groups have reported on the *N188S* mutation in Gaucher disease, involving 16 patients in total. Among these 16 patients, four were free of neurologic signs. The *N188S* mutation was first suggested as a possible neuroprotective factor in Gaucher disease by Kim et al., in the way that the *N370S* mutation works in Caucasians [1]. Kim et al. [1] studied three patients with Gaucher disease: one *N188S* homozygote, and two siblings with *N188S/L444P*. At the time of that report, the three patients did not exhibit neurologic signs, and were diagnosed as manifesting type 1 Gaucher disease. Another Chinese patient with a diagnosis of type 1 Gaucher disease also manifested *N188S/L444P* [9]. However, more recent studies described *N188S* carriers who developed neurologic signs, including myoclonus [2,3,8-10]. For example, 4 of 16 patients with myoclonus carried *N188S* in a study by Park et al. [3]. Their genotypes were *N188S/RecNciI* (two patients), *N188S/84GG* (one patient), and *N188S*/recombinant allele (one patient). Another patient with myoclonus carrying *N188S* was reported by Filcamo et al. [4]; that patient was heterozygous with *S107L* [4]. All five patients presented general seizures as well as myoclonus, and four patients exhibited abnormalities in their electroencephalograms. Other reports described three patients whose seizures had not been specified [6,7]. Although the numbers of patients are too low to prove that *N188S* leads to myoclonus, the possibility should not be ignored. One speculation, based on documented cases, contends that when *N188S* is paired with a null mutation such as *D409H* or *RecNciI*, the phenotypes become severe, and this finding is not dependent on ethnicity. This correlation was also seen in our patient, who deteriorated progressively. She carries *N188S/G199D*, and *G199D* is a null mutation which has almost no enzyme activity. However, to support this speculation, it is necessary to follow the clinical courses of heterozygotes with *N188S* and null mutations, or *N188S* and mutations with a mild effect.

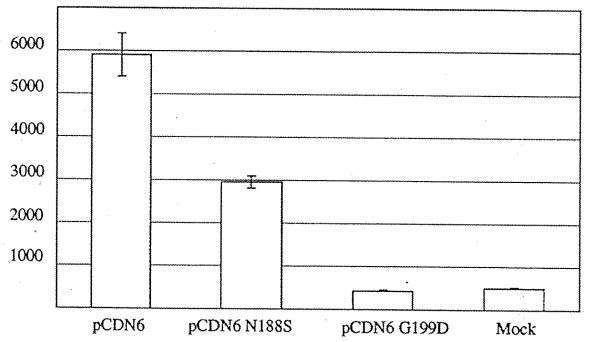

Figure 2. Glucocerebrosidase activity of the mutant proteins (nmol/hr/mg).

Montfort et al. suggested that the *N188S* mutation is a modifier variant [8]. They found three Spanish patients with a double mutant allele of *N188S* and *E326K*. In their in vitro study using a baculovirus expression system, the residual activity of *N188S+E326K* bearing glucocerebrosidase was lower than that of the *E326K*-bearing enzyme. The same effect was evident regarding *E326K* toward *N188S*. It is well-known that residual enzyme activity does not predict the severity of a phenotype in patients with Gaucher disease. However, the function of each mutation, and not residual activity, may affect the phenotypes of Gaucher disease. Therefore, more careful genetic analysis is important in detecting accurate genotypes of patients with Gaucher disease.

Our patient had manifested repeated exacerbations and remission of high fever without any clear signs of infection since age 18 years. Supranuclear gaze palsy was more distinct in the vertical position than in the horizontal position in this patient. The patient's cognitive ability may have been compromised. However, we think that the supranuclear gaze palsy had occurred horizontally and vertically. It would have been more informative if a biopsy had been available to detect any pathologic changes, as suggested by Conradi et al. [11]. The patient's central nervous system involvement progressed slowly, and her generalized convulsions increased. Unfortunately, she was unable to walk and became bedridden until her death at age 19 years.

In conclusion, we detected a novel mutation, *G199D*, with significantly low glucocerebrosidase activity. Although a correlation between *N188S* and myoclonus epilepsy cannot be established yet, it is strongly conceivable,

in light of our patient as well as previous reports. Moreover, the *N188S* mutation should be closely studied as a modifier gene that could affect the phenotype of a patient.

The authors thank Yoshikatsu Eto, MD, PhD, for his supervision, and Ms. Sayoko Iizuka for excellent technical assistance. This work was supported by a Grant for Research on Measures for Intractable Diseases from the Japanese Ministry of Health, Welfare, and Labor (2004-2006).

References

[1] **Kim** JW, Liou BB, Lai MY, Ponce E, Grabowski GA. Gaucher disease: Identification of three new mutations in the Korean and Chinese (Taiwanese) populations. Hum Mutat 1996;7:214-8.

[2] **Kowarz** L, Goker-Alpan O, Banerjee-Basu S, et al. Gaucher mutation *N188S* is associated with myoclonic epilepsy. Hum Mutat 2005;26:271-3.

[3] **Park** JK, Orvisky E, Tayebi N, et al. Myoclonic epilepsy in Gaucher disease: Genotype-phenotype insights from a rare patient subgroup. Pediatr Res 2003;53:387-95.

[4] **Filocamo** M, Mazzotti R, Stroppiano M, Grossi S, Dravet C, Guerrini R. Early visual seizures and progressive myoclonus epilepsy in neuronopathic Gaucher disease due to a rare compound heterozygosity (*N188S*/ *S107L*). Epilepsia 2004;45:1154-7.

[5] **Ida** H, Iwasawa K, Kawame H, Rennert OM, Maekawa K, Eto Y. Characteristics of gene mutations among 32 unrelated Japanese Gaucher disease patients: Absence of the common Jewish *84GG* and *1226G* mutations. Hum Genet 1995;95:717-20.

[6] **Ida** H, Rennert OM, Kawame H, Maekawa K, Eto E. Mutation prevalence among 47 unrelated Japanese patients with Gaucher disease: Identification of four novel mutations. J Inherit Metab Dis 1997;20:67-73.

[7] **Ida** H, Rennert OM, Iwasawa K, Kobayashi M, Eto Y. Clinical and genetic studies of Japanese homozygotes for the Gaucher disease *L444P* mutation. Hum Genet 1999;105:120-6.

[8] **Montfort** M, Chabas A, Vilageliu L, Grinberg D. Functional analysis of 13 GBA mutant alleles identified in Gaucher disease patients: Pathogenic changes and "modifier" polymorphisms. Hum Mutat 2004;23: 567-75.

[9] **Choy** FY, Zhang W, Shi HP, et al. Gaucher disease among Chinese patients: Review on genotype/phenotype correlation from 29 patients and identification of novel and rare alleles. Blood Cells Mol Dis 2007;38: 287-93.

[10] **Erdos** M, Hodanova K, Tasko S, et al. Genetic and clinical features of patients with Gaucher disease in Hungary. Blood Cells Mol Dis 2007;39:119-23.

[11] **Conradi** N, Kyllerman M, Månsson JE, Percy AK, Svennerholm L. Late-infantile Gaucher disease in a child with myoclonus and bulbar signs: Neuropathological and neurochemical findings. Acta Neuropathol (Berl) 1991;82:152-7.

Epilepsy & Seizure
Journal of Japan Epilepsy Society
Vol.3 No.1 (2010) pp.192-198

Case Report

Epileptic focus in a case of subcortical band heterotopia: SISCOM and ictal EEG findings

Kenjiro Kikuchi, M.D. [1)2)] Shin-ichiro Hamano, M.D. [1)], Fumihiro Goto, M.D.[1)],
Akira Takahashi, R.T. [3)], Hiroyuki Ida, M.D. [2)]

[1]Division of Neurology, Saitama Children's Medical Center, 2100 Magome, Iwatsuki-ku, Saitama-city, Saitama 339-8551, Japan
[2]Department of Pediatrics, Jikei University School of Medicine, 3-25-8 Nishi-Shinbashi, Minato-ku, Tokyo 105-8471, Japan
[3]Department of Radiology, Saitama Children's Medical Center, 2100 Magome, Iwatsuki-ku, Saitama-city, Saitama 339-8551, Japan

Key words: antiepileptic drugs, carbamazepine, zonisamide, mechanism of action, calcium-induced calcium releasing systems

Published online November 10, 2010

Abstract

We presented an 11-month-old-girl with subcortical band heterotopia who had focal epilepsy detected by subtraction single photon emission computed tomography (SPECT) co-registered to magnetic resonance (MR) imaging (SISCOM) and ictal electroencephalogram. She manifested cluster of partial seizures composed of asymmetric tonic posturing accompanied by head rotation to the right side. Ictal electroencephalogram showed that paroxysmal discharges were generated from the right parieto-occipital area and spread to sur-

Corresponding author: Kenjiro Kikuchi, M.D., Division of Neurology, Saitama Children's Medical Center, 2100 Magome, Iwatsuki-ku, Saitama-city, Saitama 339-8551, Japan.
Phone: +81-48-758-1811; Fax: +81-48-758-1818; E-mail: kikuchi.kenjiro@pref.saitama.lg.jp

rounding areas. SISCOM revealed hyperperfusion in the overlying cortex of the right superior temporal gyrus, which corresponded to the onset area of ictal epileptiform discharges. These neurofunctional findings corresponded to her clinical seizures. Her seizures were controlled by high-dose phenobarbital therapy. We considered that the patient had focal epilepsy and that the epileptic focus might be in the overlying cortex, but not in the subcortical band.

Introduction

Subcortical band heterotopia (SBH) is a rare neuronal migration disorder, which shows ectopic gray matter separated from the overlying cortex by white matter. Patients with SBH have been reported to have intractable epilepsies and mental retardations [1, 2]. These patients may present with either generalized epilepsies or focal epilepsies [2]. The epilepsies are usually evaluated by ictal and/or interictal electroencephalogram (EEG), and are rarely diagnosed by ictal single photon emission computed tomography (SPECT) or subtraction ictal SPECT coregistered to magnetic resonance (MR) imaging (SISCOM). To our knowledge, there are no reports on SISCOM evaluation of SBH during infancy. Here we report an 11-month-old girl with SBH who was diagnosed with focal epilepsy by SISCOM and ictal EEG.

Case report

An 11-month-old girl was admitted to our hospital because of intractable seizures persisting for 2 weeks. The perinatal and familial histories of the patient were unremarkable. Neurological examinations showed hypotonia in her lower extremities. She was able to sit by herself at 10 months, but could not crawl or stand up by herself at that time. Her seizures were characterized by asymmetric tonic posturing for 30 seconds accompanied by head rotation to the right side, which occurred 4 to 6 times per day.

Interictal EEG demonstrated irregular spike-and-waves and 3-4 Hz high-voltage slow waves (HVS) in the left centro-parieto-occipital area. As background EEG activities, low amplitude (20-30 μV) fast waves (30 Hz) were found in the right hemisphere. Brain MRI revealed a thin overlying cortex and an excessive band of subcortical gray matter, which was split by white matter from the frontal to the occipital region (Fig. 1). Bilateral occipital cortical surfaces were smooth and agyri. These abnormal findings were compatible with diffuse subcortical band heterotopia. Mutation in the DCX gene (178A>G) was found in exon 2.

Her seizure frequencies increased from 4-6 times per day to 4-5 times per hour, despite treatment with valproate. Ictal EEG demonstrated 3-4 Hz high-voltage slow (HVS) waves and sharp waves in the left centro-parieto-temporal area, which subsided and then 14-15 Hz fast activities with 90 μV amplitude appeared in the right mid-temporal area (Fig. 2A). These fast discharges propagated to surrounding areas and their amplitude

increased (Fig. 2B). They were followed by 5-6 Hz high voltage polymorphic discharge burst for about 20 seconds (Fig. 2C), and then 1-2 Hz HVS waves in the right hemisphere for 40 seconds (Fig. 2D). Finally these 1-2 Hz HVS discharges terminated and sharp waves reappeared in left centro-temporal area, similar to the interictal EEG findings mentioned above (Fig. 2E). The total duration of ictal activities was 75 seconds. Clinical manifestation of her seizures was recognized 30 seconds after the 14-15 Hz fast activities appeared.

Technetium-99m-ethyl cysteinate dimmer (ECD) was used for ictal SPECT. The patient was injected with 185 MBq 99m-Tc-ECD immediately after clinical seizure began, and the seizures lasted for 45 seconds after ECD injection. After ictal SPECT examination, she was given high-dose phenobarbital (PB) therapy by rectal suppository at an initial dose of 30 mg/kg/day for the first two days, followed by a dose of 20 mg/kg/day for 2 days, 10 mg/kg/day for 2 days, then 10 mg/kg/day by oral administration for the sequential consecutive days. Her seizures disappeared after PB therapy.

Interictal ECD-SPECT was performed after the disappearance of seizures. To elucidate the ictal hyperperfusion regions, we used the SISCOM analysis. The SISCOM images demonstrated hyperperfusion in the overlying cortex of the right superior temporal gyrus (Fig. 3), which corresponded to ictal EEG findings.

The patient had no seizures for more than 3 months after high-dose PB therapy, and was able to crawl and stand up by herself at the last follow-up.

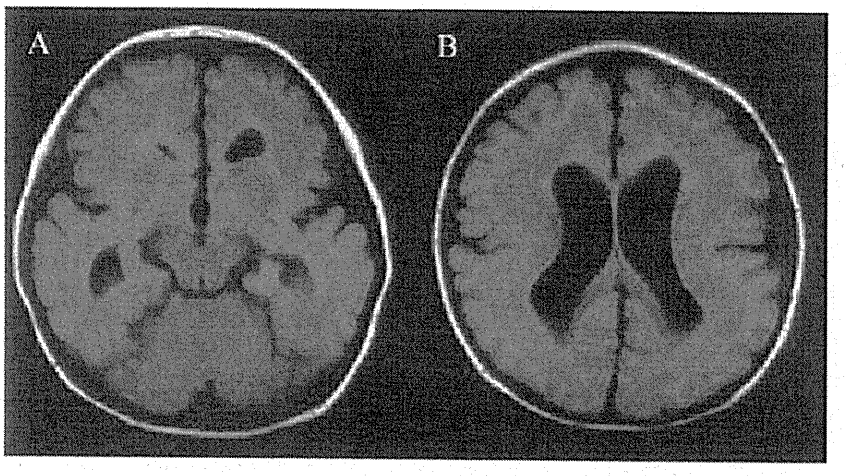

Fig. 1. Axial T1-weighted magnetic resonance (MR) imaging

Axial T1-weighted images show diffuse subcortical heterotopic gray matter and mild pachygyria.

A. At the level of cerebral peduncle.

B. At the level of body of the lateral ventricle.

Discussion

We performed SISCOM and ictal EEG on an infant with SBH. Ictal EEG indicated that the ictal paroxysmal discharges originated from the right temporal region. SISCOM showed that the hyperperfusion area corresponded to the site of onset of ictal paroxysmal discharges, and that this hyperperfusion area seemed to be corresponded to the overlying cortex of the right superior temporal gyrus. To our knowledge, this is the first report of SISCOM analysis in infant with SBH.

Some experimental studies in SBH rat models reported the correlation between

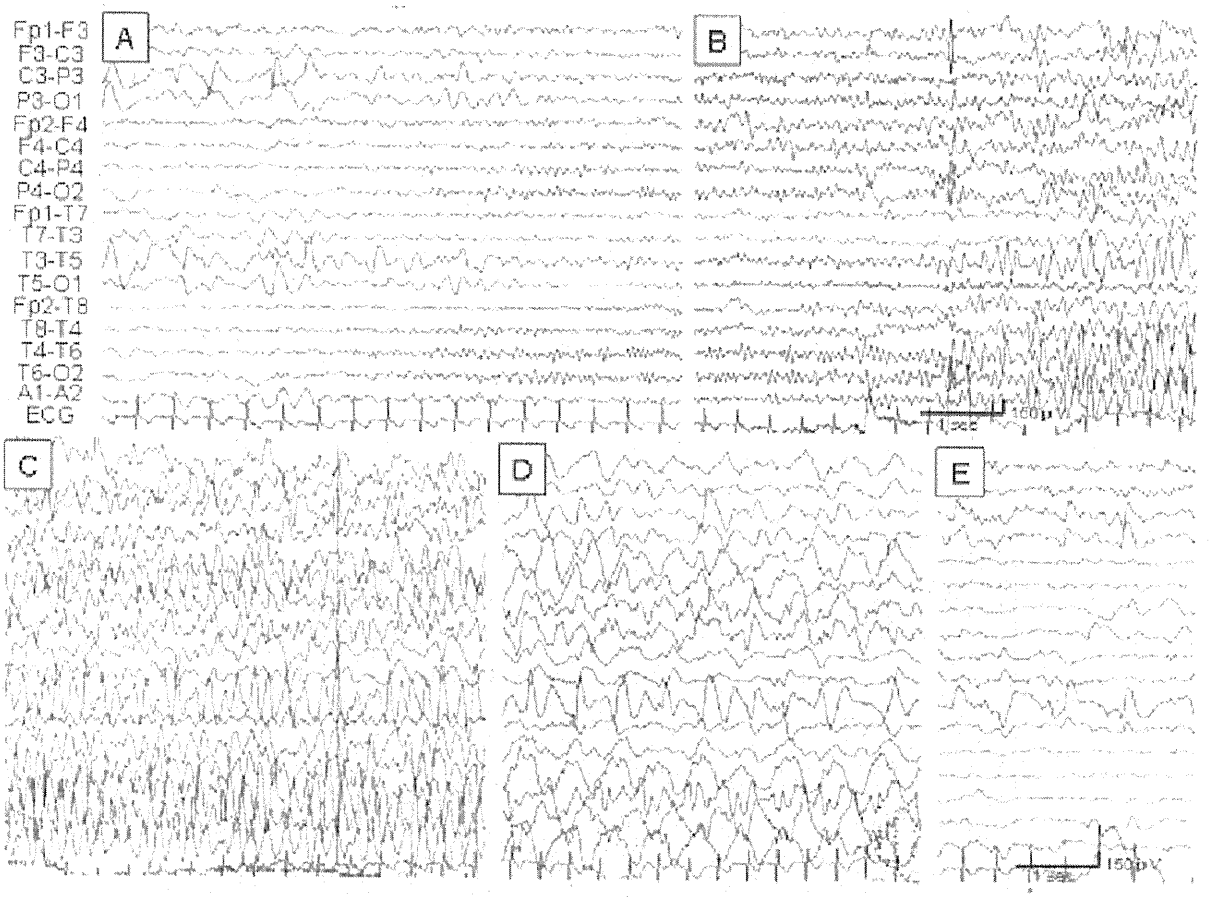

Fig. 2. Ictal electroencephalogram at the age of 11 months

(A) 3-4 Hz high-voltage slow (HVS) waves and sharp waves are found in the left centro-parieto-temporal area. The HVS disappeared and burst of 14-15 Hz fast waves is observed in the right mid-temporal area.

(B) At 10 seconds after onset, fast waves have generalized and the amplitude increases.

(C) At 15 seconds after onset, 5-6 Hz high voltage polymorphic discharges burst for about 20 seconds.

(D) From 35 seconds after onset, 1-2 Hz HVS waves in the right hemisphere persist for 40 seconds.

(E) At 75 seconds after onset, HVS waves terminate and sharp waves remain in the left centro-temporal area.

overlying cortex and subcortical band. Chen et al. [3] concluded that normotopic neurons were responsible for initiating seizures in the dysplastic neocortex, because normotopic neurons were more likely to exhibit epileptiform activity than heterotopic neurons, and heterotopic neurons were recruited into spiking by activity initiated in normotopic neurons. These observations are consistent with our findings.

Ictal SPECT has the potential to localize the ictal onset zone accurately in a noninvasive manner, and is particularly useful in MRI-negative localized epilepsy and focal cortical dysplasias [4]. Furthermore, SISCOM is useful to define the onset site of seizure [5, 6]. To our knowledge, this is the first report of SISCOM finding of SBH in infant. SISCOM images showed that the hyperperfusion area corresponded to the onset region of the ictal EEG discharges, and that this region was located in the overlying cortex. These results show that the overlying cortex may be the epileptic focus in our SBH patient.

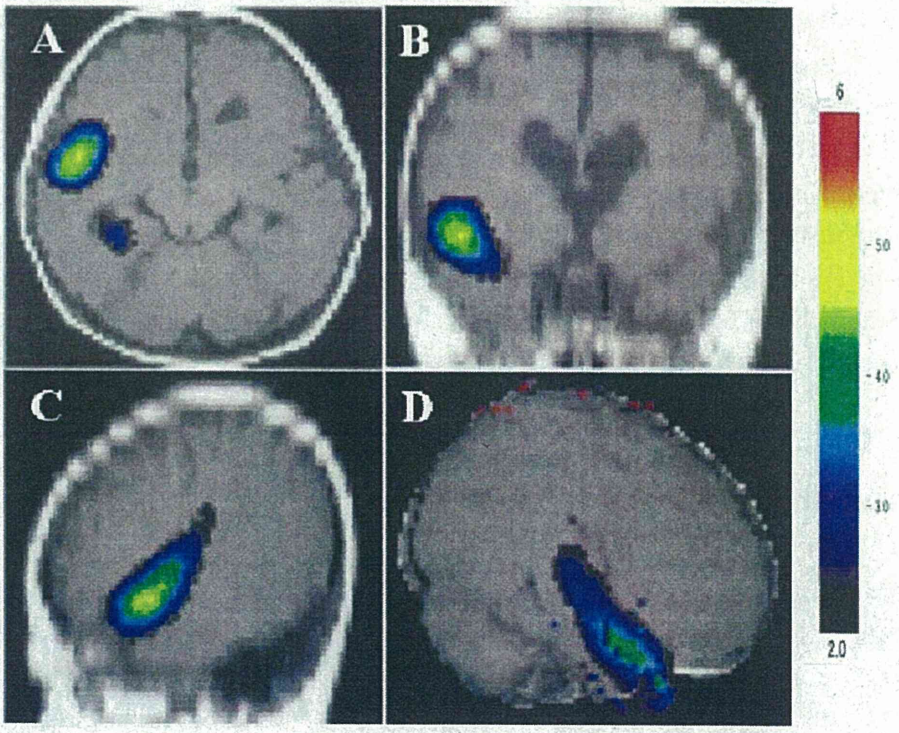

Fig 3. Subtraction ictal single-photon emission computed tomograpghy (SPECT) coregistered to magnetic resonance (MR) imaging (SISCOM)

(A) In axial view, hyperperfusion is observed in the right frontotemporal area and right medial occipitotemporal area. (B) Coronal view. (C) Sagittal view. (D) Right lateral view. (B)-(D) show that hyperperfusion is located in the right superior temporal gyrus.

Surgical treatment has been performed on focal epilepsy patients with SBH. Bernasconi et al. [7] reported that five of eight patients had no significant improvement by surgical treatment and that temporal resection resulted in especially poor outcome. They suggested that SBH might have a multifocal generator due to widespread structural abnormality, even though clinical and neurofunctional studies proved the existence of focal epileptogenic lesions. Mai et al. [8] reported that one patient with SBH had good outcome by resection of the posterior third of the middle and inferior temporal gyri and part of the fusiform gyrus. However, both groups could not explain the mechanism of seizure generation related to the normal overlying cortex and the subcortical band. Our findings suggest that surgical treatment including corticectomy will be a therapeutic option for patients with SBH.

We demonstrated symptomatic focal epilepsy using SISCOM and ictal EEG in a pediatric patient with SBH, and speculated that the overlying cortex may be the epileptic focus.

Acknowledgement

We would like to thank Dr. Mitsuhiro Kato (Yamagata University School of Medicine) for analyzing the DCX gene, and Emeritus Professor Eric Johnson (Jichi Medical University, Tochigi, Japan) for his assistance with the preparation of the manuscript.

References

[1] Barkovich AJ, Guerrini R, Battaglia G, Kalifa G, N'Guyen T, Parmeggiani A, Santucci M, Giovanardi-Rossi P, Granata T, D'Incerti L. Band heterotopia: correlation of outcome with magnetic resonance imaging parameters. Ann Neurol 1994;36:609-17.

[2] Palmini A, Andermann F, Aicardi J, Dulac O, Chaves F, Ponsot G, Pinard JM, Goutières F, Livingston J, Tampieri D, Andermann E, Robitaille Y. Diffuse cortical dysplasia, or the 'double cortex' syndrome: The clinical and epileptic spectrum in 10 patients. Neurology 1991;41:1656-62.

[3] Chen ZF, Schottler F, Bertram E, Gall CM, Anzivino MJ, Lee KS. Distribution and initiation of seizure activity in a rat brain with subcortical band heterotopia. Epilepsia 2000;41:493-501.

[4] Van Paesschen W. Ictal SPECT. Epilepsia 2004;45(Suppl.4):35-40.

[5] O'Brein TJ, So EL, Mullan BP, Hauser MF, Brinkmann BH, Bohnen NI, Hanson D, Cascino GD, Jack CR, Sharbrough FW. Subtraction ictal SPECT co-registered to MRI improves clinical usefulness of SPECT in localizing the surgical seizure focus. Neurology 1998; 50:445-54

[6] Véra P, Kaminska A, Cieuta C, Hollo A, Stiévenart JL, Gardin I, Ville D, Mangin JF, Plouin P, Dulac O, Chiron C. Use of subtraction ictal SPECT co-registered to MRI for optimizing the localization of

seizure foci in children. J Nucl Med 1999;40:786-92

[7] Bernasconi A, Martinez V, Rasa-Neto P, D'Agostino D, Bernasconi N, Berkovic S, MacKay M, Harvey AS, Palmini A, Costa da Costa J, Paglioli E, Kim HI, Connolly M, Olivier A, Dubeau F, Andermann E, Guerrini R, Whisler W, de Toledo-Morrell L, Morrell F, Andermann F. Surgical resection for intractable epilepsy in 'double cortex' syndrome yields inadequate results. Epilepsia 2001;42:1124-9.

[8] Mai R, Tassi L, Cossu M, Francione S, Lo Russo G, Garbelli R, Ferrario A, Galli C, Taroni F, Citterio A, Spreafico R. A neuropathological, stereo-EEG, and MRI study of subcortical band heterotopia. Neurology 2003;60:1834-8.

Dominant-Negative Mutations in α-II Spectrin Cause West Syndrome with Severe Cerebral Hypomyelination, Spastic Quadriplegia, and Developmental Delay

Hirotomo Saitsu,[1,*] Jun Tohyama,[2] Tatsuro Kumada,[3] Kiyoshi Egawa,[3] Keisuke Hamada,[4] Ippei Okada,[1] Takeshi Mizuguchi,[1,17] Hitoshi Osaka,[5] Rie Miyata,[6] Tomonori Furukawa,[3] Kazuhiro Haginoya,[7] Hideki Hoshino,[8] Tomohide Goto,[9] Yasuo Hachiya,[10] Takanori Yamagata,[11] Shinji Saitoh,[12] Toshiro Nagai,[13] Kiyomi Nishiyama,[1] Akira Nishimura,[1] Noriko Miyake,[1] Masayuki Komada,[14] Kenji Hayashi,[15] Syu-ichi Hirai,[15] Kazuhiro Ogata,[4] Mitsuhiro Kato,[16] Atsuo Fukuda,[3] and Naomichi Matsumoto[1,*]

A de novo 9q33.3-q34.11 microdeletion involving *STXBP1* has been found in one of four individuals (group A) with early-onset West syndrome, severe hypomyelination, poor visual attention, and developmental delay. Although haploinsufficiency of *STXBP1* was involved in early infantile epileptic encephalopathy in a previous different cohort study (group B), no mutations of *STXBP1* were found in two of the remaining three subjects of group A (one was unavailable). We assumed that another gene within the deletion might contribute to the phenotype of group A. *SPTAN1* encoding α-II spectrin, which is essential for proper myelination in zebrafish, turned out to be deleted. In two subjects, an in-frame 3 bp deletion and a 6 bp duplication in *SPTAN1* were found at the initial nucleation site of the α/β spectrin heterodimer. *SPTAN1* was further screened in six unrelated individuals with WS and hypomyelination, but no mutations were found. Recombinant mutant (mut) and wild-type (WT) α-II spectrin could assemble heterodimers with β-II spectrin, but α-II (mut)/β-II spectrin heterodimers were thermolabile compared with the α-II (WT)/β-II heterodimers. Transient expression in mouse cortical neurons revealed aggregation of α-II (mut)/β-II and α-II (mut)/β-III spectrin heterodimers, which was also observed in lymphoblastoid cells from two subjects with in-frame mutations. Clustering of ankyrinG and voltage-gated sodium channels at axon initial segment (AIS) was disturbed in relation to the aggregates, together with an elevated action potential threshold. These findings suggest that pathological aggregation of α/β spectrin heterodimers and abnormal AIS integrity resulting from *SPTAN1* mutations were involved in pathogenesis of infantile epilepsy.

Introduction

West syndrome (WS) is a common infantile epileptic syndrome characterized by brief tonic spasms, an electroencephalogram pattern called hypsarrhythmia, and mental retardation.[1] Brain malformations and metabolic disorders can be underlying causes of WS, but many cases remain etiologically unexplained.[1] Only two causative genes, *ARX* (MIM *300382) and *CDKL5* (MIM *300203), are mutated in a subset of familial and sporadic X-linked WS cases (ISSX1 and ISSX2 [MIM #308350 and #300672]).[2–4] Early infantile epileptic encephalopathy with suppression-burst (EIEE) is the earliest form of infantile epileptic syndrome.[5,6] The transition from EIEE to WS occurs in 75% of individuals with EIEE, suggesting a common pathological mechanism between these two syndromes.[5,6] We have recently reported that de novo mutations of *STXBP1* (MIM *602926) cause EIEE.[7]

Spectrins are submembranous scaffolding proteins involved in the stabilization of membrane proteins.[8,9] Spectrins are flexible and long molecules consisting of α and β subunits, which are assembled in an antiparallel side-by-side manner into heterodimers. Heterodimers form by end-to-end tetramers integrating into the membrane cytoskelton.[8,9] The spectrin repertoire in humans includes two α subunits and five β subunits. Defects of erythroid α-I and β-I spectrins and neuronal β-III spectrin are associated with hereditary spherocytosis (SPH3 and SPH2 [MIM

[1]Department of Human Genetics, Yokohama City University Graduate School of Medicine, 3-9 Fukuura, Kanazawa-ku, Yokohama 236-0004, Japan; [2]Department of Pediatrics, Epilepsy Center, Nishi-Niigata Chuo National Hospital, 1-14-1 Masago, Nishi-ku, Niigata 950-2085, Japan; [3]Department of Physiology, Hamamatsu University School of Medicine, 1-20-1 Handayama, Hamamatsu 431-3192, Japan; [4]Department of Biochemistry, Yokohama City University Graduate School of Medicine, 3-9 Fukuura, Kanazawa-ku, Yokohama 236-0004, Japan; [5]Division of Neurology, Clinical Research Institute, Kanagawa Children's Medical Center, 2-138-4 Mutsukawa, Minami-ku, Yokohama 232-8555, Japan; [6]Department of Pediatrics, Tokyo Kita Shakai Hoken Hospital, 4-17-56 Akabanedai, Kita-ku, Tokyo 115-0053, Japan; [7]Department of Pediatrics, Tohoku University School of Medicine, 1-1 Seiryo-machi, Aoba-ku, Sendai 980-8574, Japan; [8]Division of Neurology, National Center for Child Health and Development, 2-10-1 Okura, Setagaya-ku, Tokyo 157-8535, Japan; [9]Department of Neurology, Tokyo Metropolitan Children's Medical Center, 2-8-29 Musashidai, Fuchu 183-8561, Japan; [10]Department of Neuropediatrics, Tokyo Metropolitan Neurological Hospital, 2-6-1 Musashidai, Fuchu 183-0042, Japan; [11]Department of Pediatrics, Jichi Medical University, 3311-1 Yakushiji, Shimotsuke, Tochigi 329-0498, Japan; [12]Department of Pediatrics, Hokkaido University Graduate School of Medicine, North 15, West 7, Kita-ku, Sapporo 060-8638, Japan; [13]Department of Pediatrics, Dokkyo Medical University, Koshigaya Hospital, 2-1-50 Minami-Koshigaya, Koshigaya, Saitama 343-8555, Japan; [14]Department of Biological Sciences, Faculty of Bioscience and Biotechnology, Tokyo Institute of Technology, 4259-B-16 Nagatsuta, Midori-ku, Yokohama 226-8501, Japan; [15]Department of Molecular Biology, Yokohama City University Graduate School of Medicine, 3-9 Fukuura, Kanazawa-ku, Yokohama 236-0004, Japan; [16]Department of Pediatrics, Yamagata University School of Medicine, 2-2-2 Iida-nishi, Yamagata 990-9585, Japan
[17]Present address: Laboratory of Biochemistry and Molecular Biology, National Cancer Institute, National Institutes of Health, Building 37, Room 6050, Bethesda, MD 20892, USA
*Correspondence: hsaitsu@yokohama-cu.ac.jp (H.S.), naomat@yokohama-cu.ac.jp (N.M.)
DOI 10.1016/j.ajhg.2010.04.013.